

Inverse methods and nuclear radii

E. F. Hefter

Institut für Theoretische Physik, Universität Hannover, 3000 Hannover, Federal Republic of Germany

M. de Llano*

Department of Physics and Astronomy, Southern Illinois University, Carbondale, Illinois 62901

I. A. Mitropolsky

Leningrad Nuclear Physics Institute, Gatchina, Leningrad, USSR

(Received 9 January 1984)

In considering spherically symmetric three-dimensional systems, inverse methods are applied to the nuclear bound-state problem. While retaining only the self-interactions of the (occupied) bound-state levels, an analytical solution is obtained for the potential. The simplest possible approximation to it corresponding to a single fictitious bound state is used to evaluate (root mean square) radii. Combining this formula with the well-known $A^{1/3}$ dependence of the nuclear radii, a new formula is obtained containing the collective binding energy effect and the one of the saturation of nuclear forces. For absolute and relative radii (of isotopes of Sn, Xe, Nd, Dy, Yb, Os, Hg, Pb, and Pu), the results compare favorably with experiment. In spite of the crude approximations made, this approach yields the typical curvature of the plot of the experimental relative radii as a function of the mass number. The extreme simplicity of the formula recommends its use for global discussions or predictions. Yet, for a correct description of the finer details it is necessary to account explicitly for shell effects and deformations.

I. MOTIVATION

Recent years have seen an increased interest in inverse methods¹ as applied to nuclear physics (see Refs. 2 and 3 and references therein). The gist of such inversion procedures is to extract from scattering data, e.g., differential cross sections and/or phase shifts, the respective scattering potentials. Generally, such investigations do not touch questions related to the bound states contained in the scattering potential (except for the case of the deuteron). Yet, there is strong evidence that, in particular for nucleon-nucleus scattering, the self-interaction of the target nucleus should provide the dominant contribution to the scattering potential. This self-interaction or self-energy is essentially the shell model potential of the target nucleus.⁴⁻⁶

Hence, it appears reasonable to expect the discrete part of the energy spectrum of the Schrödinger operator to contain at least as much useful information as its continuum. This leads to the notion of applying inverse methods to the nuclear bound state problem⁷ to evaluate the shell model potential, U , and charge and mass densities of the respective nuclei. We do not intend to elaborate on the formalism as such, but we would like to use its simplest possible approximation in a semiphenomenological discussion of nuclear (charge rms) radii.

In a preliminary paper⁸ it has been indicated that the most primitive approximation to the approach leads to

$$\begin{aligned} \Delta R^2(B) &\equiv \langle r^2(A) \rangle - \langle r^2(A_0) \rangle \\ &= 0.777M \left[\frac{1}{B(A)} - \frac{1}{B(A_0)} \right], \quad M \equiv \hbar^2/2m \end{aligned} \quad (1)$$

for the rms radii of nuclei with mass numbers A and A_0 and with binding energies per nucleon $B=B(A)$ and $B_0=B(A_0)$, respectively. Writing the term in square brackets in the form

$$-[B(A) - B(A_0)]/B(A)B(A_0)$$

and noting that the denominator is almost constant for different isotopes of a nucleus, it is recognized⁸ that (1) corresponds to a relation which Gerstenkorn⁹ proposed 15 years ago—but on purely phenomenological grounds. In spite of its simplicity, (1) turned out to be highly useful^{10,11} and even provided the basis for predictions that were later confirmed by experiment.¹⁰ But, alas, there are also many cases in which it fails.

A similar statement is appropriate as far as the application of the famous global relation

$$\begin{aligned} R(A) &\equiv \langle r^2(A) \rangle^{1/2} = \sqrt{3/5} \hat{R}(A) \equiv \sqrt{3/5} r_0 A^{1/3} \\ r_0 &= 1.2 \text{ fm} \end{aligned} \quad (2)$$

to the discussion of relative radii is concerned. Equation (2) arises due to rather general considerations based on the saturation of nuclear forces. It leads directly to

$$\Delta R^2(A) = \frac{3}{5} r_0^2 [A^{2/3} - A_0^{2/3}] = 0.864 [A^{2/3} - A_0^{2/3}]. \quad (3)$$

This relation is also very useful and it works reasonably well for a variety of isotope sequences, but it too fails for quite a large number for nuclei.

A common feature of (1) and (3) is that they both ignore deformations and shell effects. Without any limitations this statement is true for (3). In the case of (1), a faint trace of these effects is evidenced through the

minute changes in the binding energies per nucleon as functions of A , yet this dependence is by far too crude to explain the experimental data correctly. It is not doubted that a formally correct and consistent description has to include these effects explicitly as, e.g., done with remarkable success in some work relying on the Hartree-Fock¹² and droplet models.¹³ Within the inverse approach, we hope to be soon in the position of treating at least shell effects adequately. However, in this paper we would like to address a different question. Equation (1) contains only the collective binding energy effect and (3) only the effect of the saturation of nuclear forces. Both of them are undoubtedly very important. Is it possible to obtain from an appropriate combination of (1) and (3) useful information which is not accessible when applying these relations separately?

To give some indications for the way in which inverse methods yield relation (1), we recall in Sec. II the gist of the method, indicate how it may be related to the

Hartree-Fock approach, and show how it yields (1). Then we combine (1) and (3). In Sec. III we try first to find out whether the emerging formula is consistent with the prominent features of absolute radii as functions of the mass number A . Then we plunge into a detailed discussion of experimental data related to relative (charge rms) radii. The final section contains a short summary.

II. BASIC FORMULAS

We cannot solve the appropriate many-body Schrödinger equation. Hence, we consider as a suitable starting point for the discussion of a stationary system the N single-particle Schrödinger equations with the N bound-state wave functions, ψ_n , and energy eigenvalues, E_n . For spherically symmetric systems, the corresponding radial equations may be cast into the form of one-dimensional (1D) equations (with $x \geq 0$) which for s waves become

$$-M\partial_{xx}\psi_n(x) + U(x)\psi_n = E_n\psi_n, \quad \partial_{xx} \equiv \partial^2/\partial x^2, \quad M \equiv \hbar^2/2m, \quad n = 1, 2, \dots, N. \quad (4)$$

(Further details on the method used and additional background information may be taken from Refs. 1, 7, and 14–17. In particular, that concerns the case with $l \neq 0$ which has been discussed for some specific situation by Ablowitz and Cornille.¹⁸ From their work it may be inferred that the characteristics of these cases are, in the simple approximation to be considered in the following, the same ones as for s waves. Hence, we discuss here only the justified s -wave approximation.)

To solve (4) with the aid of inverse methods, the required input data are the N bound-state energy eigenvalues and additional data related to the continuum. The emerging solution, $U(x)$, may symbolically be written as the sum of two terms, i.e., $U(x) = U_c(x) + U_N(x)$, where the indices c and N refer to the continuum and to the N bound states, respectively. $U(x)$ cannot be given in a closed form. However, if we include only the self-interactions of the N occupied (ground-state) levels in our considerations, then the analytical solution $U(x) = U_N(x)$ is obtained:^{1,7,14–17}

$$\begin{aligned} U_N(x) &= \sum_{j=1}^N [-4\sqrt{-E_j M} \psi_j^2(x)] \\ &= \sum_{j=1}^N -4\sqrt{-E_j M} \rho_j(x) = 2M\partial_{xx}[\ln(\det F)], \\ F_{ij} &= \delta_{ij} + 2\sqrt{f_i f_j} / (\sqrt{-E_i} + \sqrt{-E_j}), \\ f_j(x) &= \sqrt{-E_j} \exp(\sqrt{-E_j/M} x). \end{aligned} \quad (5)$$

(In the 1D case with $-\infty < x < \infty$ this solution U_N corresponds to N reflectionless potentials for which an incident wave packet is for all energies transmitted without any reflection.) From (5) it is readily appreciated that the N energy eigenvalues E_j uniquely determine the total potential $U_N(x)$, wave functions $\{\psi_j(x) | j = 1, 2, \dots, N\}$, densities ρ_j , and total density $\rho \equiv \sum \rho_j$.

The approximation $U \cong U_N$, i.e., the restriction to the self-energy of the respective system, has been shown to be a good approximation to finite¹⁵ (e.g., a Gaussian, the clipped harmonic oscillator) and infinite¹⁶ (e.g., the harmonic oscillator) potentials. In addition, it has been proved that the self-interactions (in 1D, reflectionless potentials) $U_N = \sum_j U_{Nj}$ provide a rapidly converging sequence of approximands to infinite potentials that diverge, for large x , like the harmonic oscillator or faster.¹⁹

Insertion of the solution (5) into the original Schrödinger equations (4) yields the nonlinear Schrödinger equation

$$-M\partial_{xx}\psi_n(x) - 4 \sum_{j=1}^N \sqrt{-E_j M} \psi_j^2 \psi_n = E_n \psi_n, \quad n = 1, 2, \dots, N. \quad (6)$$

It is well known that (6) corresponds exactly to the Hartree-Fock (HF) equations with two-body Skyrme forces.²⁰ However, within the HF the implied restriction to contact interactions between pairs of particles is obviously a rather drastic one. On the other hand, the U_N of (5) has been shown to be a fairly accurate approximation to the complete potential;^{15,16,19} hence, we may nourish the hope that this approach possibly has a richer dynamical content.

To come closer to our goal, the derivation of (1) from inverse methods, i.e., from (4) and (5), let us recall that the characteristic feature of all the individual contributions ρ_j to the total density is that the amplitude, ρ_0 , appears again in the respective form factor. This is best illustrated for the case $N=1$ with

$$\begin{aligned} \rho(x) = \rho_1(x) &= \sqrt{-E/4M} \operatorname{sech}^2(\sqrt{-E/M} x) \\ &\equiv \rho_0 \operatorname{sech}^2(2\rho_0 x); \quad \rho_0 \equiv \sqrt{-E/4M}, \end{aligned} \quad (7)$$

where we suppressed for the sake of simplicity the index "1." Note that the sech^2 form factor is asymptotically related to the Gaussian, f_G , and Saxon-Woods, f_{SW} , form factors since

$$\begin{aligned} \text{sech}^2(x) &\rightarrow 1 - x^2 + \dots = \exp(x^2) = f_G(x) \quad x \ll 1 \\ &\rightarrow 4/[1 + \exp(2x)] = 4f_{SW}(x) \quad x \gg 1 \end{aligned} \quad (8)$$

holds where nuclear physicists commonly use $x = (r - r_0)/a$. Hence, it is apparently not unreasonable to attempt to approximate in a crude way the density distributions of nuclei by (7). But in view of the fact that (7) cannot really be expected to come close enough to a Saxon-Woods form factor to be realistic for the density distributions of heavy nuclei like lead, it appears more sensible to concentrate on the respective relative radii.

Identifying in such a sense a single contribution to the total density in an approximate way with a whole nucleus implies, of course, that we should in (7) no longer use a single energy eigenvalue for E , but instead the corresponding averaged quantity. Recently²¹ the well-known single-particle sum rule

$$B(A) = \frac{1}{2A} \sum_{i=1}^N n_i(t_i + E_i)$$

due to the Hartree-Fock approach has been shown to lead to

$$B(A) \cong \frac{0.35}{A} \sum_{i=1}^N n_i E_i .$$

(The n_i , t_i , and E_i are the degeneracy, average kinetic energy, and energy eigenvalue of the i th state, respectively.) The summation is to be performed over all occupied proton and neutron levels separately.) From the mathematical structure and the physical content of these relations it appears most appropriate to identify the binding energy per nucleon, $B(A) < 0$, with the energy E required in (7). To avoid confusion we henceforth use $B(A)$ in place of this energy.

The half-width at half-maximum radius and rms radius of (7) yield almost exactly the same expression, namely,

$$\begin{aligned} R(B) \equiv R(B(A)) &= \frac{1}{2}\rho_0^{-1} \cosh^{-1} \sqrt{2} \\ &= 0.4406/\rho_0 = 0.88\sqrt{M/B(A)} \\ &= 4.04/\sqrt{B(A)} . \end{aligned} \quad (9)$$

Taking the square of this $R(B)$ and then the difference between $R^2(B)$ and $R^2(B_0) \equiv R^2(B(A_0))$, we immediately arrive at (1), i.e., the desired expression.

Equations (1) and (9) are only expected to give information in respect to relative radii. As stated in the Introduction, we would like to combine (2) and (9) to account simultaneously for the geometry effects arising from the saturation of the nuclear forces and for the collective binding energy effect. For that purpose we define with the aid of (9) the relative radius

$$R_r(B) \equiv R(B(A))/R(B(\text{av})) = \sqrt{B(\text{av})/B(A)} , \quad (10)$$

where "av" = "average" refers to a suitable reference nucleus (which may be taken to be a specific one or a fictitious average one) and $B(\text{av})$ to its binding energy per nucleon. The obvious combination of (10) with (2) then yields

$$\begin{aligned} R(A, B) &\equiv R(A)R_r(B) = \sqrt{3/5}r_0 A \sqrt{B(\text{av})/B(A)} \\ &= \sqrt{-3B(\text{av})/5}r_0 \frac{A^{1/3}}{\sqrt{-B(A)}} \end{aligned} \quad (11)$$

and [with $B(\text{av}) = -8.5$ MeV as given in textbooks and $r_0 = 1.2$ fm]

$$\begin{aligned} \Delta R^2(A, B) &= \frac{3B(\text{av})}{5} r_0^2 \left[\frac{A^{2/3}}{B(A)} - \frac{A_0^{2/3}}{B(A_0)} \right] \\ &= 7.34 \left[\frac{A^{2/3}}{B(A)} - \frac{A_0^{2/3}}{B(A_0)} \right] . \end{aligned} \quad (12)$$

Equation (11) may now be used to obtain global information on the absolute radii as functions of A , combined with some local deviations due to (collective) binding energy effects. Since the total binding energies $B_t = AB(A)$ are very well known,²² this means that the resulting predictions or estimates will contain no adjustable parameters, provided r_0 and the average binding energy per nucleon $B(\text{av})$ are given. We shall use the standard values $r_0 = 1.2$ fm and $B(\text{av}) = -8.5$ MeV.

Before discussing the numerical work designed to test the use of (12) in respect to the simpler relations (1) and (3), it should be recalled that, because of the way in which these relations have been derived, and in view of the averaged input to be used, there are some obvious limitations on their range of applicability, namely:

- (i) Shell effects (which are well known to manifest themselves in the experimental data²³) and pairing correlations are not accounted for.
- (ii) The existence of deformed nuclei is ignored.
- (iii) No distinction is made between mass and charge distributions.

III. NUMERICAL DISCUSSION

Computing with the aid of (11) the *absolute radii* $R(A, B)$ for nuclei throughout the periodic table leads, for medium and heavy nuclei, to rather small deviations from the $A^{1/3}$ dependence of (2). But the changes go in the right direction, bringing about a slightly improved correspondence of calculated radii with experiment. This is due to the collective binding energy effects. Yet, from rather general considerations and from a closer look at the resulting numbers, it is inferred that $B(\text{av})$ should take on different values for different regions of the periodic table. In this spirit the choices $B(\text{av}) = -8$ MeV for $A > 90$ and $B(\text{av}) = -9.75$ MeV for $A < 90$ would lead to an even closer agreement of computations with experiment. Yet, due to the absence of a formal justification for specific values of $B(\text{av})$, we believe it to be more honest to retain the textbook value of -8.5 MeV and to introduce an empirical renormalization constant N_{AB} into (11), i.e.,

$$R(A, B) \equiv \sqrt{N_{AB}} 2.71 A^{1/3} / \sqrt{-B(A)} .$$

The deviations of (11) from (2) should be most pronounced in regions of the mass table in which the binding energy per nucleon varies more rapidly with the mass number, say, for $1p$ -shell nuclei with $5 \leq A \leq 16$. The respective experimental data taken from (Ref. 24) are given by the crossed open circles in Fig. 1. The full curves at the top, $R = r_0 A^{1/3}$, and at the bottom, $\langle r^2 \rangle^{1/2} = \sqrt{3/5} R$, both fail to reproduce the fine structure of the data, though they do give the correct global trend. The results of an older rather detailed analysis (based on proton binding energies and Coulomb energies)²⁵ do much better (full points with error bars). The numbers based on (11) as multiplied by $\sqrt{N_{AB}} = 1.033$ are depicted by the dotted open circles. In view of the simplicity of (11), the nice agreement with the experimental trend is certainly of note. Yet, the minor discrepancies observed in Fig. 1 are already a clear indication that neglect of deformations and shell effects in (11) must necessarily make this relation fail in some cases.

Summarizing the results of this discussion of absolute radii we have seen that (2) (containing the geometry effect due to the saturation of nuclear forces) yields essentially the correct global trend of the nuclear radii as functions of the mass numbers (i.e., a well-known result); however, supplementing it by the collective effect of the binding energy, (11), gives rise to a definite improvement in the otherwise too monotonous local behavior of the radii. This is rather obvious for light nuclei where $B(A)$ varies rapidly with A .

From the above we infer that (11) brings us in general closer to experiment than (2), while (9) is apparently completely unable to make any predictions in respect to absolute nuclear radii. Turning to a discussion of relative radii, we would therefore expect in a similar way varying degrees of success for relations (12), (3), and (1). Starting with (12) this expectation seems to be confirmed by rather

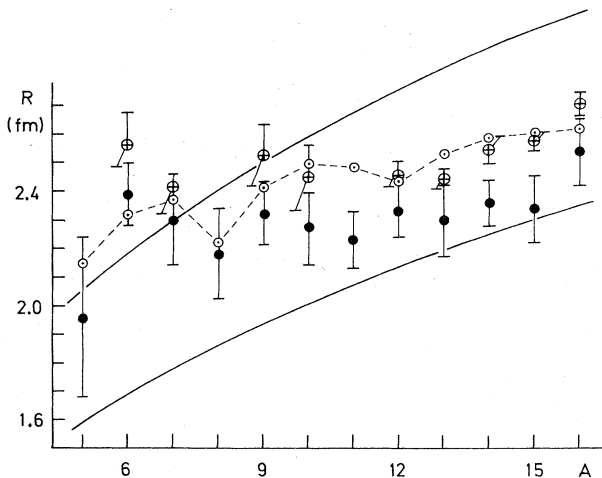


FIG. 1. The dots with error bars representing $R = \langle r^2 \rangle^{1/2}$ are taken from the analysis of Ref. 25. More recent experimental points (Ref. 24) are given by open circles with crosses. The two full curves illustrate the global trends predicted by the simple $A^{1/3}$ dependences: $R = r_0 A^{1/3}$ (upper curve) and $R = \sqrt{3/5} r_0 A^{1/3}$ (lower curve) with $r_0 = 1.2$ fm. The dotted open circles are (11) multiplied by 1.033.

general arguments: As a rule the differences in the mass numbers are expected to be larger than the ones in the respective binding energies; hence, the latter should provide only a second order effect. This reasoning is not invalidated by the knowledge that there are many real nuclei which prefer to follow the trend predicted by the latter, i.e., by (1) (Refs. 9–11). After all, shell effects and deformations which are *not* accounted for by *any* of these relations are in some cases quite important²³ and they should be expected to give rise to rather drastic deviations from these simple formulas. A further point which should be borne in mind is that experiment yields the differences between nuclear radii, i.e., the ΔR^2 , to a much higher accuracy than the absolute radii.

Let us first apply (1) and (12) to a discussion of the measured isotope shifts related to different isotopes of Sn, Hg, and Pb; later we shall also have a look at other cases. In Fig. 2 the relative (charge) radii ΔR^2 for the tin isotopes are plotted versus the mass number A . With the exception of two data points, the agreement between experiment (dots) and the calculations (full curves) based on (12) is good. On the other hand, the dashed curve corresponding to (1) yields by far more structure than observed in the experimental data. The odd-even staggering in this curve is very pronounced and does *not* correspond to the specific one observed in experiment. The effect of the additional $A_j^{2/3}$ appearing in (12) has obviously smoothed out the structure, thus improving the agreement to experiment.

The behavior of the mercury isotopes as a function of A (Fig. 3) requires greater effort to accomplish a theoretical explanation.^{24,11b} Moreover, this case appears to be of increased interest, since a comparison is possible with results based on the interacting boson model (IBM).²⁷ In that work by Barfield *et al.* it is said that: "The four Hamiltonian parameters which were allowed to vary freely from isotope to isotope were found to be consistent with the corresponding IBM parameters for platinum and osmium. Overall, the calculated energy spectra and electromagnetic properties are in reasonable agreement with experiment." The isotope shift data treated in Ref. 27 are

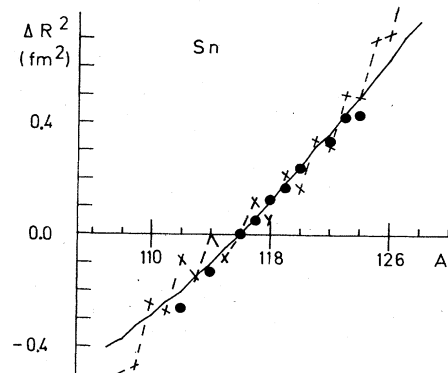


FIG. 2. Referring to the nucleus ^{116}Sn , the experimental points adopted from Ref. 26 (dots) are put in relation to the results of (1) multiplied by $N_B = 3.16$ (dashed curve) and of (12) multiplied by $N_{AB} = 0.678$ (full curve); $r_0 = 1.2$ fm and $B(\text{av}) = -8.5$ MeV.

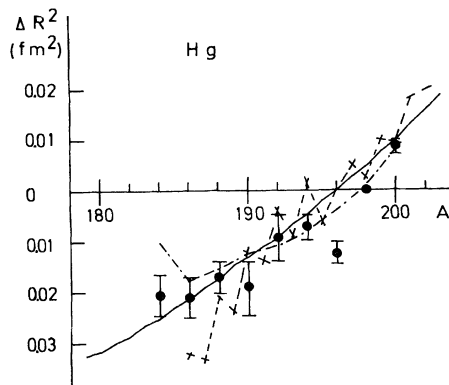


FIG. 3. Experimental data for Hg isotopes from Ref. 28 are shown as dots and IBM calculations (Ref. 27) as a dot-dashed curve. The full curve is (12) multiplied by $N_{AB}=0.149$ and the dashed one is (1) multiplied by $N_B=1.054$; $r_0=1.2$ fm and $B(av)=-8.5$ MeV.

taken from the work of Bonn *et al.*²⁸ and shown in Fig. 3 as dots with error bars. The dot-dashed curve corresponds to the IBM results. The full curve is (12) multiplied by $N_{AB}=0.149$. It would appear that a chi-squared analysis might show that both IBM and Eq. (12) do equally well or poorly. As in the case of the Sn isotopes (Fig. 2), we note in Fig. 3 that for mercury the simple binding energy relation (1) (dashed curve) yields a richer structure than the full curve. But again the odd-even staggering is not of the type observed experimentally. As before, we note that the smoothing of the curve due to the effect of the geometric constants $A_j^{2/3}$ leads globally to a definite improvement. This holds in spite of the fact that most of the structure is lost.

Since (12) should be most reasonable for spherically symmetric nuclei, it is convenient that we can refer to a recent study²⁹ of the relative radii of the lead isotopes, where new experimental data are presented together with a discussion in terms of the liquid drop model and Hartree-Fock calculations. For a more detailed comparison the data are given in the form of a figure (Fig. 4) and tabulated (Table I). The dots in Fig. 4 represent the experimental data,²⁹ while the dashed and dot-dashed curves, respectively, are calculations within the liquid drop model and the Hartree-Fock (with Skyrme III forces). From the figure it is seen that to a first approximation the overall trend is reproduced by either of the theoretical approaches. However, a qualitative difference between the HF and droplet approaches and the present one, i.e., (12), is that the former apparently predict a global dependence of ΔR^2 on A which is close to a straight line, while the inverse method yields a curve which is slightly concave upwards, thus much better reflecting the trend followed by experiment. A look at Table I confirms this: In all cases relation (12) with its combined A and B dependences yields a closer (or in some cases just equally good) agreement with experiment than the liquid drop model. Only for three points do the Hartree-Fock calculations do better than (12). The last column, containing

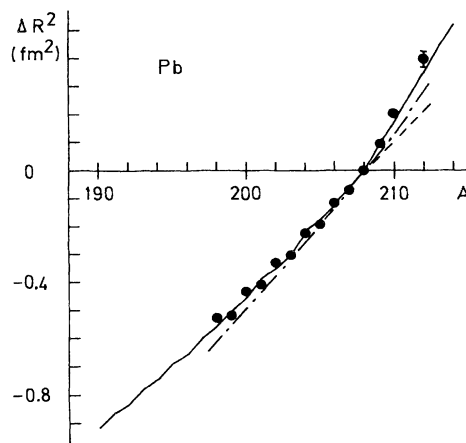


FIG. 4. Since part of the data have also been given in Table I, see the caption there. The dots refer to experiment (Ref. 29), while dashed, dot-dashed, and full curves correspond, respectively, to calculations within the liquid drop model, HF with Skyrme III forces (Ref. 29), and (12) times $N_{AB}=0.711$; $r_0=1.2$ fm and $B(av)=-8.5$ MeV.

numbers based on (1), shows that this simple formula (with the appropriate choice for N_B) yields a fair agreement with experiment for $A > 208$, but fails for $A < 208$.

To arrive at a more complete and better understanding

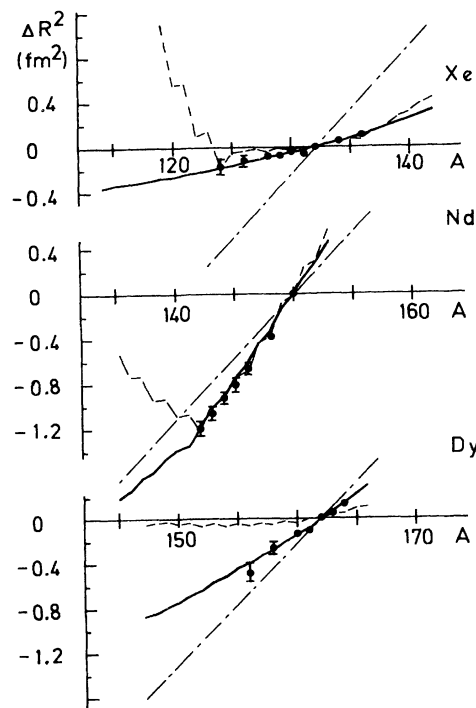


FIG. 5. Referring to the isotopes ^{132}Xe , ^{150}Nd , and ^{162}Dy , the respective experimental data (points) taken from Ref. 26 are put in relation to the $\Delta R^2(A,B)$ of (12) (multiplied by $N_{AB}=0.2$, 0.55, and 1.0, respectively; see full curves), to the $\Delta R^2(A)$ of (3) ($N_A=1$; dot-dashed lines), and to the $\Delta R^2(B)$ of (1) (multiplied by $N_B=10$, 52, and 13, respectively; see broken curves); $r_0=1.2$ fm and $B(av)=-8.5$ MeV.

of the working of relations (1), (3), and (12), let us now consider a few more cases as displayed in Figs. 5 and 6. Charge and mass numbers of the nuclei considered in these two figures range from $Z=54$ to 94 and from $A=114$ to 246, respectively. The only criterion for their selection was the desire to cover a wide range of charge and mass numbers, thus allowing us to bridge the gap between the data discussed so far. Some of the experiments as, e.g., the ones for Nd, show a steep slope, while there are also cases exhibiting rather smooth and small changes of ΔR^2 as a function of the mass number. In line with the preceding discussion it is observed that the $\Delta R^2(A)$ of relation (3), which contain only the geometry effect due to the saturation of nuclear forces, yield a straight line. Of course, in most cases these lines would reproduce the global trend of the experimental data, provided they are appropriately normalized (i.e., rotated around the origin; but we used for all of them $N_A=1$). However, this relation certainly does not make the slightest attempt to reproduce the fine structure of the data.

$\Delta R^2(B)$ [see (1)], on the other hand, yields in most cases by far too much structure and curves that are in general too concave. The limited amount of experimental data contained in the figures does not allow us to decide uniquely against the strong "bending" of $\Delta R^2(B)$ as a real physical effect. But in particular the cases of Dy (see the bottom of Fig. 5) and of Yb (the top of Fig. 6) do indicate that these effects are grossly overestimated by relation (1).

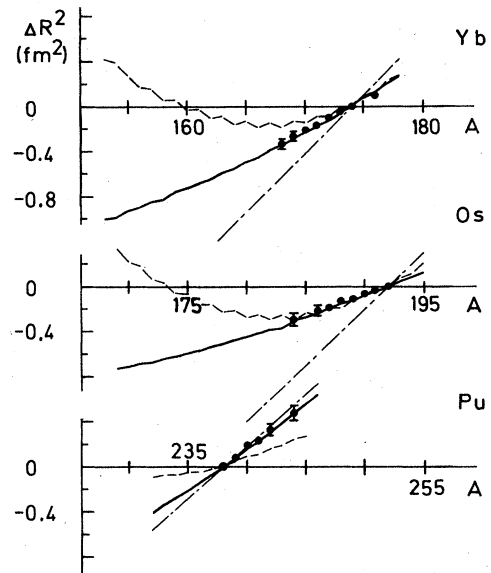


FIG. 6. Essentially the same as Fig. 5, but this time for the nuclei Yb, Os, and Pu with the reference isotopes ^{174}Yb , ^{192}Os , and ^{238}Pu . The respective normalization constants for $\Delta R^2(A,B)$ are $N_{AB}=0.475$, 0.31, and 0.56; for $\Delta R^2(A)$ they are in all cases unity, and for $\Delta R^2(B)$ they are given by $N_B=27$, 28, and 15.5; $r_0=1.2$ fm and $B(\text{av})=-8.5$ MeV.

TABLE I. For several lead isotopes ($Z=82$) the squared relative radii are given with ^{208}Pb as the reference nucleus. Except for the last two columns these data have been taken from Ref. 29. SIII, droplet model, and experimental data refer, respectively, to calculations within the Hartree-Fock method, the droplet model, and the experiment. The next to last column contains the $\Delta R^2(A,B)$ predicted by (12) times $N_{AB}=0.711$ [$r_0=1.2$ fm; $B(\text{av})=-8.5$ MeV]. The last column relies on (1) as multiplied by $N_B=2.133$ with r_0 and $B(\text{av})$ as before.

Pb A	$\Delta R^2 \equiv R^2(A) - R^2(208)$ (fm ²)				
	HF (SIII)	Droplet model	Experiment	$\Delta R_B^2(A)$	$\Delta R^2(B(A))$
192				-0.7999	15.0
193				-0.7474	15.4
194				-0.7146	4.8
195				-0.6618	4.8
196				-0.6277	-4.6
197				-0.5725	-3.6
198	-0.606	-0.54	-0.528(11)	-0.5352	-11.2
199	-0.548	-0.48	-0.518(6)	-0.4792	-8.8
200	-0.489	-0.42	-0.432(8)	-0.4381	-14.1
201	-0.430	-0.37	-0.409(4)	-0.3802	-10.9
202	-0.370	-0.32	-0.330(4)	-0.3366	-15.1
203	-0.310	-0.27	-0.303(4)	-0.2759	-10.4
204	-0.249	-0.21	-0.224(3)	-0.2296	-13.0
205	-0.187	-0.16	-0.195(4)	-0.1671	-6.7
206	-0.125	-0.11	-0.118(1)	-0.1180	-8.3
207	-0.063	-0.05	-0.072(2)	-0.0559	-2.5
208	0	0	0	0	0
209	0.060	0.05	0.091(5)	0.0893	19.9
210	0.138	0.11	0.202(14)	0.1664	33.3
211	0.207	0.16		0.2566	53.7
212	0.276	0.21	0.398(27)	0.3340	67.0
213				0.4259	87.7
214				0.5030	101.4

This tentative suggestion is seemingly supported by studies of the $\Delta R^2(B)$ dependence as given in the literature.⁸⁻¹¹ However, it should be borne in mind that the number of data considered here is too small to provide conclusive evidence for this notion.

A comparison between the slopes of the $\Delta R^2(A)$ lines and the $\Delta R^2(A,B)$ curves shows clearly that most of the latter (except for the one related to Dy) have been renormalized by multiplication with the numbers given in the figure captions. The predictions of $\Delta R^2(A,B)$, (12), agree nicely with experiment. Except for the normalization constant N_{AB} added "by hand," there is no adjustable parameter in this relation. Obviously the good correspondence to experiment is due to the fact that the binding energies contained in (12) add some structure to the $\Delta R^2(A)$ curves, (3), and bend them a bit so that they follow the global trend of the experimental data. In such a way (12) provides a vivid illustration for the real significance of the simple relation $\Delta R^2(B)$ originally proposed by Gerstenkorn.⁹ The most obvious cases supporting this remark are possibly the ones of Nd, Dy, Os, and Pu. But except for the nuclei Nd and Os, a different normalization of the $\Delta R^2(B)$ curves would help very much to show that more directly (we refrained from doing so since that would also have the side effect of making it rather difficult for the reader to distinguish the different curves). Yet, the case of Nd, Fig. 5, illustrates this point quite nicely. The isotopes of Sn, Fig. 2, and of Os, Fig. 6, reveal another—this time unpleasant—feature, i.e., all the curves produced do predict an odd-even staggering, but in most cases it goes in the wrong direction. This failure of the otherwise rather convincing predictions of (12) is a bit disappointing. Yet, it has to be borne in mind that (12) is extremely simple and that it does not contain any adjustable parameter, except for the renormalization constant N_{AB} which has been added "by hand." To determine N_{AB} we need in principle only a single experimental value ΔR^2 for a specific nucleus. All the other $\Delta R^2(A,B)$ are then predictions. Hence, (12) already gives us quite a lot. In view of its simplicity and of the averaged input used, it is no surprise that it fails in the finer details. E.g., within the context of the above average relations, nuclei with almost identical average binding energies per nucleon—which may have rather different shell structures—are to yield

exactly the same results. Hence, we are automatically led to the need to incorporate shell effects in more accurate calculations, e.g., in the complete formula (5) with the appropriate single-particle energies. Eventually deformations will also have to be included.

IV. SUMMARY

It has been recalled that application of inverse methods to the solution of the nuclear mean field Schrödinger eigenvalue problem yields for the self-interactions of the bound states an analytical solution for the mean field U . Exploiting the characteristics of this solution, the one-level approximation to it has been shown to lead to useful information related to absolute and relative nuclear (charge) radii; see in particular (11) and (12). The predicted (relative) radii for nuclei ranging from $A=110$ to 245 have been compared to experimental data as determined, e.g., via optical methods.^{9-11,24,26,28,29} At least for Pb and Hg the quality of the results is no worse than that of the liquid drop model, the Hartree-Fock, and the interacting boson model calculations. The typical bending of the plots of experimental data versus the mass number is (in contrast to quite a few other approaches) nicely predicted. The major advantage of the relation given, (12), is that it is an extremely simple analytical formula containing no free parameter, yet, in most cases it has to be renormalized by multiplication with the constant N_{AB} .

The results of this simple approximation to (5) give rise to the hope that application of inverse methods to the nuclear bound-state problem may indeed prove useful in providing additional insight into the rather complicated quantum mechanical many-body problem posed by the atomic nucleus. Further work attempting to account appropriately for the shell structure of the respective nuclei is still in progress.

ACKNOWLEDGMENTS

E.F.H. is very grateful for the hospitality extended to him during his stays at IFUNAM (Mexico) and at the LNPI (Leningrad). M. de L. appreciates partial support by CONACyT, ININ and DAAD.

*On leave from Instituto de Física-UNAM, 01000 México, D.F. México.

¹K. Chadan and P. C. Sabatier, *Inverse Problems in Quantum Scattering Theory* (Springer, New York, 1977); R. G. Newton, *Scattering Theory of Waves and Particles* (Springer, New York, 1982).

²A. M. Kobos and R. S. Mackintosh, *Ann. Phys. (N.Y.)* **123**, 296 (1979); M. Münchow and W. Scheid, *Phys. Rev. Lett.* **44**, 1299 (1980); R. A. Baldock, B. A. Robson, and R. F. Barrett, *Nucl. Phys.* **A366**, 270 (1981).

³R. Lipperheide and H. Fiedeldey, *Z. Phys. A* **301**, 81 (1981); R. Lipperheide, S. Sofianos, and H. Fiedeldey, *Phys. Rev. C* **26**, 770 (1982).

⁴M. Bauer, E. Hernández-Saldana, P. E. Hodgson, and J. Quintanilla, *J. Phys. G* **8**, 525 (1982); C. Mahaux and H. Ngô,

Phys. Lett. **100B**, 285 (1981).

⁵M. Kohno and D. W. L. Sprung, *Nucl. Phys.* **A397**, 1 (1983); M. Kohno, D. W. L. Sprung, S. Nagata, and N. Yamaguchi, *Phys. Lett.* **137B**, 10 (1984).

⁶E. F. Hefter, *Phys. Lett.* **141B**, 5 (1984).

⁷E. F. Hefter and K. A. Gridnev, *Z. Naturforsch.* **38A**, 813 (1983); E. F. Hefter, *Acta Phys. Pol.* **A65**, 377 (1984), and references therein.

⁸E. F. Hefter and I. A. Mitropolsky, *Z. Naturforsch.* **39A**, 603 (1984).

⁹S. Gerstenkorn, *C. R.* **268B**, 1636 (1969); **272B**, 110 (1971).

¹⁰S. Gerstenkorn, *Comments At. Mol. Phys.* **9**, 1 (1979).

¹¹(a) R. Wenz, E. Matthias, H. Rinneberg, and F. Schneider, *Z. Phys. A* **295**, 303 (1980); (b) H. H. Stroke, in *Atomic Physics*, edited by I. Lindgren, A. Rosén, and S. Svanberg (Plenum,

- New York, 1983), p. 509.
- ¹²X. Campi and M. Epherre, *Phys. Rev. C* **22**, 2605 (1980).
- ¹³W. D. Myers and K.-H. Schmidt, *Nucl. Phys.* **A410**, 61 (1983).
- ¹⁴I. Kay and H. E. Moses, *J. Appl. Phys.* **27**, 1503 (1956); P. D. Lax, *Comm. Pure Appl. Math.* **21**, 467 (1968); C. S. Gardner, J. M. Greene, M. D. Kruskal, and R. M. Miura, *Phys. Rev. Lett.* **19**, 1095 (1974).
- ¹⁵P. Asthana and A. N. Kamal, *Z. Phys. C* **19**, 37 (1983).
- ¹⁶J. F. Schonfeld, W. Kwong, J. L. Rosner, C. Quigg, and H. B. Thacker, *Ann. Phys. (N.Y.)* **128**, 1 (1980).
- ¹⁷E. B. Plekhanov, A. S. Suzko, and B. N. Zakhariev, *Ann. Phys. (Berlin)* **39**, 313 (1982).
- ¹⁸M. J. Ablowitz and H. Cornille, *Phys. Lett.* **72A**, 277 (1979).
- ¹⁹I. Sabba-Stefanescu, *J. Math. Phys.* **23**, 2190 (1982).
- ²⁰M. de Llano, *Nucl. Phys.* **A317**, 183 (1979); E. F. Hefter, *Prog. Theor. Phys.* **69**, 329 (1983).
- ²¹E. F. Hefter and I. A. Mitropolsky, Leningrad Nuclear Physics Institute Report 860, 1983.
- ²²A. H. Wapstra and K. Bos, *At. Data Nucl. Data Tables* **19**, 177 (1977).
- ²³I. Angeli and M. Csatlós, *Nucl. Phys.* **A288**, 480 (1977).
- ²⁴R. C. Barrett and D. F. Jackson, *Nuclear Sizes and Structure* (Clarendon, Oxford, 1979).
- ²⁵D. H. Wilkinson and M. E. Mafethe, *Nucl. Phys.* **85**, 97 (1966).
- ²⁶K. Heilig and A. Steudel, *At. Data Nucl. Data Tables* **14**, 613 (1974).
- ²⁷A. F. Barfield, B. R. Barrett, K. A. Sage, and P. D. Duval, *Z. Phys. A* **311**, 205 (1983).
- ²⁸J. Bonn, G. Huber, H.-J. Kluge, and E. W. Otten, *Z. Phys. A* **276**, 203 (1976).
- ²⁹R. S. Thompson, M. Anselment, K. Bekk, S. Göring, A. Hauser, G. Meisel, H. Rebel, G. Schatz, and B. A. Brown, *J. Phys. G* **9**, 443 (1983).